AD-A066 082 CALIFORNIA UNIV LOS ANGELES DEPT OF MATERIALS F/G 11/6
MAGNETOMECHANICAL ACOUSTIC EMISSION OF IRON AND STEELS.(U)
JAN 79 K ONO, M SHIBATA N00014-75-C-0419
UNCLASSIFIED TR-79-01 NL

1 OF 1
ADA
066082

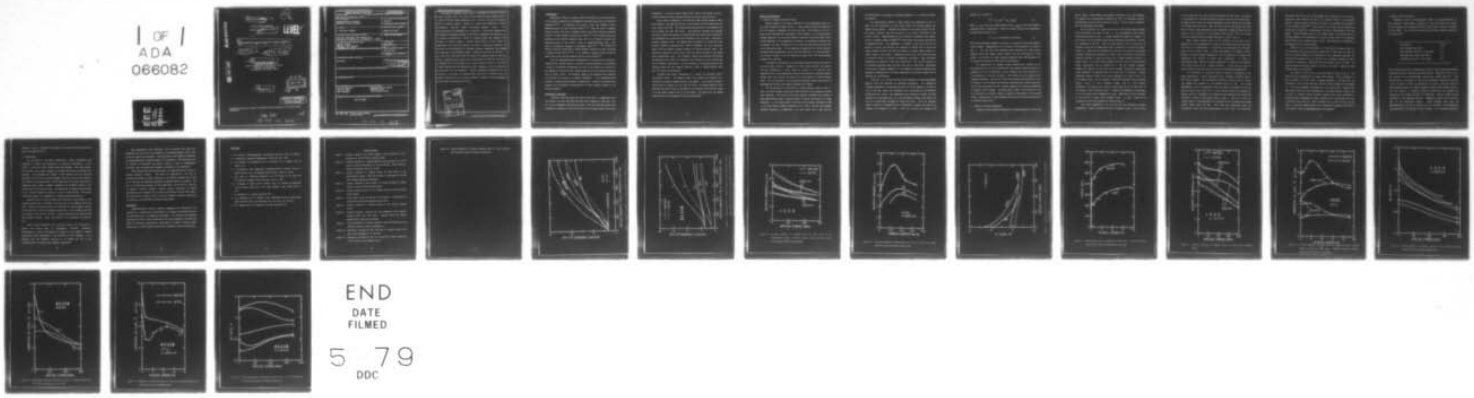

END
DATE
FILMED
5 79
DDC

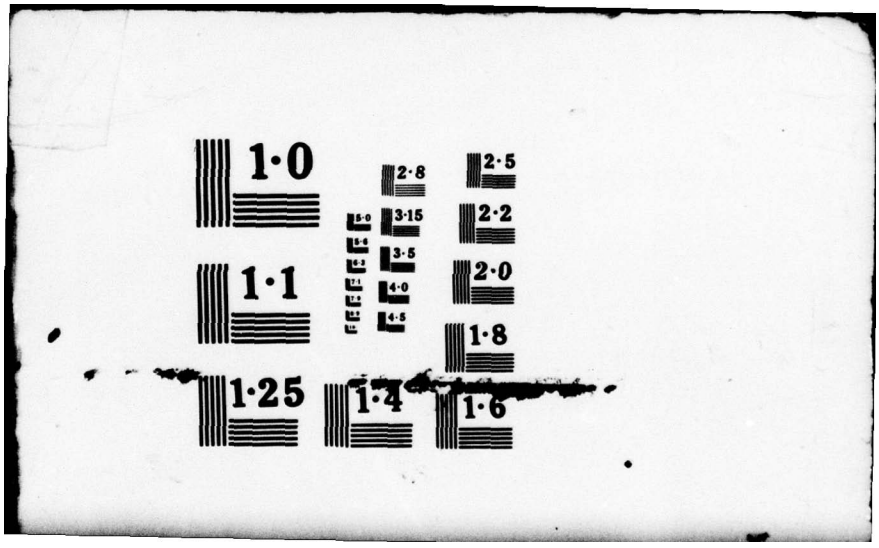
1·0
1·1
1·25
1·4
1·6
1·8
2·0
2·2
2·5
2·8
3·15
3·5
4·0
4·5

AD A066082

DDC FILE COPY

(9) Technical Report No. 79-01

to the

Office of Naval Research

Contract No. (15) N00014-75-C-0419

LEVEL II

(6) MAGNETOMECHANICAL ACOUSTIC EMISSION OF IRON AND STEELS.

(12) 29 p.

(14) TR-79-01

(10) Kanji Ono and M. Shibata
Materials Department
School of Engineering and Applied Science
University of California
Los Angeles, California 90024

DDC
RECEIVED
MAR 27 1979
A

(11) January 1979

DISTRIBUTION STATEMENT A
Approved for public release;
Distribution Unlimited

Reproduction whole or in part is permitted for any purpose of the United States Government.

406 237

79 03 26 013

SECURITY CLASSIFICATION OF THIS PAGE (When Data Entered)

REPORT DOCUMENTATION PAGE

READ INSTRUCTIONS BEFORE COMPLETING FORM

1. REPORT NUMBER: ONR Technical Report No. 79-01
2. GOVT ACCESSION NO.:
3. RECIPIENT'S CATALOG NUMBER:

4. TITLE (and Subtitle): Magnetomechanical Acoustic Emission of Iron and Steels
5. TYPE OF REPORT & PERIOD COVERED: Technical
6. PERFORMING ORG. REPORT NUMBER:

7. AUTHOR(s): K. Ono and M. Shibata
8. CONTRACT OR GRANT NUMBER(s): N00014-75-C-0419

9. PERFORMING ORGANIZATION NAME AND ADDRESS: Materials Department, 6531 Boelter Hall, University of California, Los Angeles, CA 90024
10. PROGRAM ELEMENT, PROJECT, TASK AREA & WORK UNIT NUMBERS:

11. CONTROLLING OFFICE NAME AND ADDRESS: Physics Program, ONR-800 N. Quincy Street, Arlington, VA 22217
12. REPORT DATE: Jan. 1979
13. NUMBER OF PAGES: 26

14. MONITORING AGENCY NAME & ADDRESS(if different from Controlling Office):
15. SECURITY CLASS. (of this report): Unclassified
15a. DECLASSIFICATION/DOWNGRADING SCHEDULE:

16. DISTRIBUTION STATEMENT (of this Report): Unlimited

DISTRIBUTION STATEMENT A
Approved for public release;
Distribution Unlimited

17. DISTRIBUTION STATEMENT (of the abstract entered in Block 20, if different from Report):

18. SUPPLEMENTARY NOTES:

19. KEY WORDS (Continue on reverse side if necessary and identify by block number):
Acoustic Emission
Iron and Steel
Heat Treatment
Magnetomechanical effect
Residual Stress
Prior Plastic Strain

20. ABSTRACT (Continue on reverse side if necessary and identify by block number):

See next page

DD FORM 1 JAN 73 1473 EDITION OF 1 NOV 65 IS OBSOLETE
S/N 0102-LF-014-6601

SECURITY CLASSIFICATION OF THIS PAGE (When Data Entered)

79 03 26 013

The motion of magnetic domain walls in ferromagnetic materials produces acoustic emission (AE). This type of AE was detected during magnetization of a nickel and during elastic loading of iron. Recently, this was also found to depend on applied stress. Varying AE outputs were observed on several ferromagnetic materials under alternating magnetic field. This magnetomechanical AE phenomenon has a potential of performing nondestructive measurements of residual stresses in structures, components and weldments, and we examined systematically effects of applied stress and magnetic field strength in ferritic steels. Several carbon steels, A 533 B steel and commercially pure iron were tested in annealed or normalized condition. By employing two AE transducers of different resonant frequencies, rms voltages were measured at two frequency ranges. Maximum stress level was 350 MPa. It was found that 1020 steel shows the highest AE response among the materials tested. Residual stress levels can be determined by monitoring the ratio of the outputs of two AE transducers for a given material condition. The amount of prior cold work and the difference in heat treatment can also be determined by monitoring this AE phenomenon. Several exploratory experiments for the developing a new method of nondestructive evaluation of residual stress and material conditions have also been conducted. Results of these experiments are described and discussed in detail.

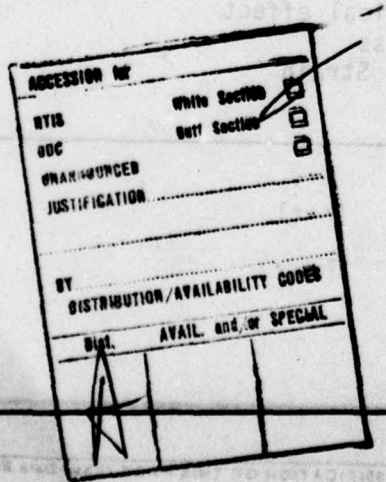

Introduction

Significant effects of stress, plastic deformation and microstructures on the magnetic properties of ferromagnetic materials have been well known and documented.[1,2] In measuring the elastic strain and residual stress, magnetostriction has been utilized widely.[3,4] When the level of applied field is varied, the shift in magnetic domain structures produces ultrasonic waves[5], of which intensity varies with stress.[6] Such ultrasonic waves are generally called acoustic emission (AE), and in the instances arising from magnetostriction, we will refer to them as "magnetomechanical AE". This effect is mechanical analogue of "Barkhausen effect".[7] The intensity of induced electrical pulses due to domain boundary movement has been correlated to applied stress level.[3,4,8] In the absence of magnetic field, AE due to domain wall motion was also observed during tensile testing.[9]

Since the magnetomechnical AE phenomenon has the potential of becoming a nondestructive testing method for residual stress determination, we conducted a series of experiments determining the level of AE signals as a function of the composition, microstructure, applied magnetic field and external stress as well as plastic strain. Two frequency ranges of AE transducers were explored to ascertain the presence of frequency dependence. A few experiments were directed to examine possible modes of applications. Results are reported here together with preliminary interpretation of their possible origins of the observed behavior.

Experimental Procedures

A series of iron and steels was used in this study. A commercially pure iron (magnet iron) and AISI 1020 steel were fully annealed at 1183 K for 1 hr. in an inert atmosphere and furnace cooled. AISI 1045 and 1065 steels were normalized by heating to 1123 K for 30 min and air-cooled (albeit in an inert

atmosphere). A low alloy steel, ASTM A 533 B, class 2, was tested in the as-received condition having tempered bainite plus ferrite microstructure.

Round tensile specimens of the half-size ASTM standard geometry (E-8) were machined. The gauge section has 6.3 mm diameter and 32 mm length and the total length was 84 mm. The threaded grip sections were 12.7 mm diameter (16 mm for magnet iron and 1020 steel). Following heat treatment and thorough cleaning, a sample was mounted in threaded grips with teflon tape lubrication. Two transducers for AE detection were attached to the flat ends. These were a resonant transducer with the nominal center frequency of 175 kHz (AC 175L, Acoustic Emission Technology Corp. (AETC), Sacramento, CA) and a miniature sensor with the nominal resonant frequency of 500 kHz (MAC-500, AETC). The former was coupled via viscous resin, while the latter was glued to the sample using cyanoacrylate ester. The transducer outputs were amplified 60 dB using preamplifiers (160, AETC) with bandpass filter plug-ins of 125 to 250 kHz and 125 to 1000 kHz, respectively. The rms voltages of the amplified outputs were measured using true rms reading voltmeters (3400 A, Hewlett-Packard, Palo Alto, CA) and an X-Y-Y'recorder.

Stressing and plastic deformation of a sample was performed using a floor-model Instron. The magnetic field on the sample was generated by a solenoid encircling the gauge section of the sample. It was powered through a variac with AC voltages of up to 140 V at 60 Hz. The maximum magnetic field generated was 2550 A/m rms at the center of the solenoid, which had the casing of 25 mm inside diameter and of 33 mm length. The sample was thus magnet longitudinally and the magnetic circuit was open-ended.

Results and Discussion

1. Effects of Magnetic Field and Stress

Typical results of AE output (referred to at the preamplifer input) vs. the field strength are shown in Fig. 1. Here, applied stress was absent and the low frequency transducer (AC 175L) was used. The intensity of AE at a given stress increased with the magnetic field strength. At the maximum field strength employed, the AE output tended to approach a saturation level, which varied depending on the composition of samples. The maximum AE intensity was the highest for 1020, followed by A 533 B, 1045 and 1065 steels and pure iron in the decreasing order. At the beginning of magnetization, the AE intensity increased almost immediately in pure iron and 1020 steel. In other materials, the initial increase in the AE intensity was small until the field strength reached 150 to 200 A/m.

An example of variation in the AE intensity-field strength curves due to stress is shown in Fig. 2. Results for A 533 B steel are given for each of the two transducers at three levels of stress, 0, 172 and 344 MPa. Significant drop in the maximum AE intensity was observed by applying external stress, which also affected the shape of the AE intensity vs. field strength curve. For this material, the AE intensity decreased rapidly with stress of approximately 100 MPa, and further decreases were limited.

The AE intensity of 1020 steel is plotted against stress in Fig. 3. Here, two field strength levels were fixed and both of the transducer outputs were indicated. The outputs of the lower frequency transducer were higher at both magnetization levels. Relative effects of stress were greater at a lower frequency. At the stress level of 140 MPa, the AE intensity decreased to 56% at 175 kHz (nominal resonant frequency) and to 75% at 500 kHz (also nominal resonant frequency) in comparison to the zero stress level. Note that the

differed between the loading and unloading segments; i.e. a hysteresis effect was present.

The compositional effects of these results are summarized in Fig. 4, where the AE intensities at three stress levels are plotted against the nominal carbon content. A maximum was observed at the carbon content of 0.2%. The result indicates that the AE output is not solely controlled by the ferrite content. Magnetomechanical AE is believed to originate from a sudden motion of magnetic domain boundary[5,6] which shifts the spatial distribution of magnetostriction. The dispersion of carbides in the ferrite matrix and mixing of ferrite and pearlite are expected to inhibit and to retard the domain boundary motion. The lower AE intensity at higher carbon levels is a direct result of this effect. Commercially pure iron is all ferrite and such an inhibition effect is limited to nonmetallic inclusions. Thus, the domain boundaries are expected to have less restrictions. Yet, the AE intensity in the observed frequency range was lower than that in 1020 steel. Differences in the size of magnetic domains or in the mobility of domain boundaries were apparently responsible for the above observation, but further studies will be required for clarification.

From Fig. 3, it can be seen that the AE responses to stress and applied magnetic field are dissimilar at different frequencies. As a measure of frequency dependence, we selected the ratio of the AE outputs at 175 kHz to that at 500 kHz, which was calculated after correcting for the different background noise levels. The background noise correction followed the usual assumption of mean-square sum; i.e., the mean-square voltage output equals the sum of the mean-square voltages of signal and noise. Since the frequency range is fixed by a transducer and the independence of signal and noise can be assured, the assumption is valid. Thus, the corrected rms voltage of AE

signals, $\bar{V}_r$, is given by

$$\bar{V}_r^2 = (V_{r,\,obs})^2 - (V_{r,\,noise})^2 \qquad (1)$$

where $V_{r,\,obs}$ is the rms voltage observed and $V_{r,\,noise}$ is the rms voltage of background noise, respectively. Using the outputs from the two transducers, we define the AE ratio, R, as

$$R = \bar{V}_r \text{ (at 175 kHz)}/\bar{V}_r \text{ (at 500 kHz)} \qquad (2)$$

The AE ratio generally depends on material, its condition, stress and magnetic field strength. Dependencies of R to stress in four materials are shown in Fig. 5. Iron and 1020 steel exhibited sharp decreases in R with stress, whereas steels with higher carbon contents had less variations in R with stress. At 100 MPa, low carbon materials produced about 50% decreased in R, in contrast to 10% drop in R for 1045 and 1065 steels.

For applications of residual stress determination, methods can be developed based on the above observations. The simplest method may rely on a comparison of the AE intensity at given frequency and field strength for a fixed geometry of the test articles. This suffers from the uncertainty of transducer coupling. The use of AE ratio can eliminate this difficulty, since a transducer can be designed with multiple resonances and a single coupling to the test piece provides the data. Another approach can utilize the dependence on magnetic field strength. As clearly shown in Fig. 2, the variation in the AE intensities at different levels of magnetic field depends on the applied stress. Combinations of these parameters should provide unique identification of residual stress level.

2. Effects of Plastic Deformation

Stress and field strength dependencies of magnetomechanical AE vary with

plastic strain. These effects were studied in 1020 and A 533 B steel samples. The samples were progressively deformed and their AE responses measured. Stress-plastic strain curves are given in Fig. 6. On the curves are markers, where AE measurements were made.

The AE intensity vs. stress curves for the 1020 steel sample deformed 18.3% plastically are shown in Fig. 7. The corresponding curves before straining were given in Fig. 3. Several significant changes are evident. At zero stress, the AE intensity after plastic deformation decreased at 175 kHz, but increased at 500 kHz. This is better shown in Fig. 8, where the AE intensity (corrected for background noise) is plotted as a function of plastic strain, ϵ_p. When the field strength was 2250 A/m, the value of $\bar{V}_r$ increased initially, followed by a decrease at 175 kHz. For $\bar{V}_r$ at 500 kHz, the increase increase continued to about 15% strain and a slight decrease occured at a higher strain. At a lower field strength (750 A/m), $\bar{V}_r$ at 175 kHz decreased almost continuously with ϵ_p, whereas $\bar{V}_r$ at 500 kHz increased slightly. Changes were smaller at the lower field strength. Simililarly complicated strain dependence is expected when the stress level is different. Another remarkable change is found in the stress dependence (cf. Figs. 3 and 7). In the annealed state, the AE intensity continually decreased with increasing tensile stress at both frequency ranges (Fig. 3). After plastic deformation, the shape of the curves at high fields and at 175 kHz (Fig. 7) was similar to that observed in Fig. 3. However, more generally, the decrease in the AE intensity was accompanied by a hump. This effect was most prominent at 500 kHz and at lower field strength levels. In fact, a peak can be recognized for the curve obtained at 1500 A/m (Fig. 7).

The stress dependence of the AE ratio was also affected by plastic deformation. Figure 9 presents the plot of R against stress. For the strain

of up to 6.5%, the R vs. stress curves were similar to each other. The values of R decreased 30 to 40% when stress was raised to near the flow stress level. At higher strain levels, the stress dependence of R was reduced and the values of R became less than unity. When the field strength was reduced from 2250 A/m to 750 A/m, these observations were essentially unchanged except that the values of R for strain up to 6.5% became lower by 10%. The R vs. stress curves at higher strains were almost identical to those of Fig. 9.

These results indicate that the AE intensity and AE ratio can be employed for the discrimination of heavily cold worked materials from those with little or no deformation. In 1020 steel, the difference can be detected, using the AE ratios, above or below approximately 10% plastic strain. However, the field strength dependence of the AE intensity can indicate more sensitively the presence of small prior deformation. In order to differentiate small amounts of plastic deformation, it appears to be essential that stress levels are not grossly different. Further work is needed to clarify whether stress and plastic strain can be determined independently.

It is important to ascertain effects of material differences on the above observations. Similar experiments were, therefore, performed using A 533 B steel samples. The stress-strain relation is given in Fig. 6. One of the samples was deformed to the maximum strain of 15%. The stress dependencies of $\bar{V}_r$ are presented in Fig. 10, where the frequency was at 500 kHz and three strain levels of 0, 1.4 and 15% were chosen for presentation. Without any prior deformation, the observed stress dependence was essentially identical to those of 1020 steel, shown in Fig. 3. With ϵ_p of 1.4%, the initial region of rapid decrease in $\bar{V}_r$ vanished and the $\bar{V}_r$-stress curve became concave upward below 200 MPa. This trend was accentuated after 15% deformation. Here, the curve became similar to that in Fig. 7 for 1020 steel,

except the rapid drop of ∇_r at low stresses was not observed in A 533 B steel. Apparently, these effects are due to the internal stress in the deformed samples. Magnetic domain structures are known to be refined by the presence of the internal stress.[2-4] This is expected to reduce the AE intensity by decreasing the magnitude of displacement step due to the movement of one such domain. Another possible cause of the observed shape of ∇_r-stress curves in deformed samples is the distribution of internal stress, which is not affected significantly by the applied elastic stress. This explains the broadening of the maximum in ∇_r at lower stresses.

Effects of ε_p on the AE intensity in A 533 B steel are shown in Fig. 11. The variations with ε_p were much more complex than in 1020 steel (cf. Fig. 8). Initial straining reduced the AE intensity at both frequencies employed. ∇_r continually decreased with ε_p at 500 kHz, but it reached a minimum at a few % followed by a maximum at 10% strain when the frequency was at 175 kHz. The observed behavior is almost opposite of that for 1020 steel. Reasons for this finding remain to be explored.

The values of the AE ratio are plotted against stress in Fig. 12. The observed stress dependencies are again quite complex. Before straining, it had a minimum at 80 MPa, while a maximum appeared at 150 MPa after 15% deformation. The R values decreased initially, then increased with increasing ε_p. This strain dependence was sensitive to the stress level. Despite these complicated stress and strain dependencies, it is again feasible based on the R value, to separate heavily deformed materials from those undeformed or deformed little. Regardless of stress, R greater than 0.85 indicates the level of plastic strain above 4%. When R exceeds 0.95, ε_p level is more than 9%. Thus, a relatively simple method can be developed to determine the level of cold working using the magnetomechanical AE phenomenon.

3. Effects of Microstructures

Preliminary tests of microstructural effects on magnetomechanical AE were conducted. Round tensile specimens of A 533 B steel were heat treated and AE responses were determined without stress using a resonant transducer (AC 750, AETC). The corrected AE intensities and heat treatment conditions are listed below.

As received	12.0 μV
Water quenched from 1200 K	1.2
Water quenched plus 873 K 1 day temper	11.9
Normalized (air cooled from 1200 K)	2.1
Normalized plus 873 K, 1 day temper	10.2

Water quenching resulted in martensitic structure, while normalizing produced essentially bainitic structure with some ferrite. Tempering at 873 K for 1 day resulted in the recrystallized ferrite plus carbide particles. This microstructure was similar to that of the as-received. Significant reduction in the AE output occurred in martensitic or bainitic structure, which is understandable because the domain boundary movement should become difficult with the presence of numerous obstacles; dislocations for quenched and dislocations and carbide particles for normalized. Internal stress may also contribute to the observed reduction. Tempering restored the AE levels to that of the as-received sample. These findings imply that the magnetomechanical AE can be utilized for the detection of microstructural variations and of the variance in heat treatment. In the hardened conditions,

however, it may be difficult to determine the residual stress because the AE level is already quite low.

4. Applications

On the basis of the above observations, several experiments were performed to explore the feasibility of practical applications. In one series, a steel weld under tensile stress was examined. Mild steel plates, 9.5 mm thick, were joined by manual arc welding and strips, 25 mm wide, were machined. Two solenoids were placed on both surfaces over the weld and energized by 60 Hz AC. The surface magnetic field was 1130 A/m rms, normal to the surface of the welded strip. The AE output was 3.2 μV after correction of background noise, using a resonant transducer (AC 750,AETC) coupled to the surface about 50 mm from the weld. The application of nominal tensile stress of up to 30 MPa reduced the output at a rate of 0.23% per MPa. This stress sensitivity appears to be adequate for residual stress determination.

Another series of tests utilized 1045 steel bolts, heat-treated to the tensile strength level of 690 MPa. The bolts were 12.7 mm diameter and 127 mm long. Using an encircling solenoid with 2250 A/m rms field strength at 60 Hz, the AE level was 7.3 μV with background correction. An AE transducer (AC 750) was coupled to one end of the bolt. Stress sensitivity was 0.29% per MPa under tensile loading. Again, this appears to be sufficient for practical use.

These results demonstrate that practical devices can be produced to measure the stress level in ferromagnetic structural components. Determination of prior cold working and fatigue is also possible. Another potentially useful application is the evaluation of heat treatment. It is expected that the frequency spectrum of AE singals can aid in the differentiation of different heat treatment conditions.

When magnetically soft materials, such as silicon iron sheet and amorphous iron alloy foil, were subjected to alternating magnetic field, very strong AE signals were produced. The monitoring of their magnetic properties via magnetomechanical AE method appears to be promising. This method also can be utilized in monitoring the texture control of some of ferromagnetic materials, since the domain wall movement is expected to be anisotropic.

These observations reported here need to be expanded further in order to develop practical devices. The means of magnetization, the use of differential methods to cancel variations in the material response and the use of AE counting and amplitude distribution analyses should be explored. The use of an encircling solenoid is often impractical, but the use of a yoke (as in magnetic particle testing) required special precaution to ensure reproducible field strength and to avoid the AE signals from the yoke itself. The orientation of magnetic field is also an important parameter, especially in relation to the detection of biaxial stress fields.

Conclusions

Magnetomechanical acoustic emission phenomenon was evaluated of its potential for nondestructive determination of residual stress,plastic strain and microstructure of ferromagnetic materials. Its intensity and frequency spectrum were found to vary sufficiently with these parameters, providing the basis for practical applications. Much effort is needed to develop useful devices and to clarify various sources that contribute to this AE phenomenon.

References

1. R.M. Bozorth, "Ferromagnetism", van Nostrand, New York, 1951, pp. 598-631.
2. S. Chikazumi, "Physics of Magnetism", Wiley, New York, 1964.
3. C.G. Gardner, G.A. Matzkanin and D. L. Davidson, Int. J. Nondest. Test. 3 (1971) 131.
4. K. Stierstadt, "Der Magnetische Barkhausen-Effekt, Springer Tracts in Modern Physics" vol. 40, Springer-Verlag, Berlin, 1966, pp. 2-106.
5. A.E. Lord, Jr., "Physical Acoustics", vol. XI, edited by W.P. Mason and R.N. Thurston, Academic Press, New York, 1975, p. 290.
6. H. Kusanagi, H. Kimura and H. Sasaki, "Proc. 1st General AE Symposium" held in Tokyo, Japan, Dec. 1977, Japan Nondest. Insp., Tokyo, 1977, p. 145.
7. H. Barkhausen, Z., Physik, 20 (1919) 401.
8. G.A. Matzkanin and C.G. Gardner, "Proc. ARPA/AFML Review of Quantitative NDE", AFML-TR-75-212, Air Force Mat. Lab., OH, 1976, pp. 791-812.
9. F.P. Higgins and S. H. Carpenter, Acta Met. 26 (1978) 133.

FIGURE CAPTIONS

Figure 1. Acoustic emission vs. applied magnetic field strength for five materials at 175 kHz without applied stress.

Figure 2. Acoustic emission vs. applied magnetic field strength for A 533 B steel at three stress levels, 0, 172 and 344 MPa. Solid lines for 500 kHz and dotted lines for 175 kHz.

Figure 3. Acoustic emission vs. applied stress for 1020 steel at two magnetization levels. Note the presence of hysteresis in the AE level during loading and unloading.

Figure 4. Acoustic emission at three levels (0, 69 and 138 MPa) vs. carbon content of iron and plain carbon steels.

Figure 5. Acoustic emission ratio, R, vs. applied stress for iron and plain carbon steels.

Figure 6. Stress-strain curves of 1020 and A 533 B steels. Circles mark the strain levels where AE measurements were made.

Figure 7. Acoustic emission vs. applied stress for 1020 steel, deformed 18.3%.

Figure 8. Acoustic emission, corrected for the background noise, against plastic strain for 1020 steel. Applied stress was absent. Magnetization levels are indicated.

Figure 9. Stress dependence of acoustic emission ratio of 1020 steel at six different levels of plastic deformation.

Figure 10. Background corrected AE level (500 kHz) vs. applied stress for A 533 B steel, deformed 0, 1.4 and 15%.

Figure 11. Background corrected AE level as a function of plastic strain for A 533 B steel at zero applied stress.

Figure 12. Stress dependence of acoustic emission ratio of A 533 B steel at five different levels of plastic deformation.

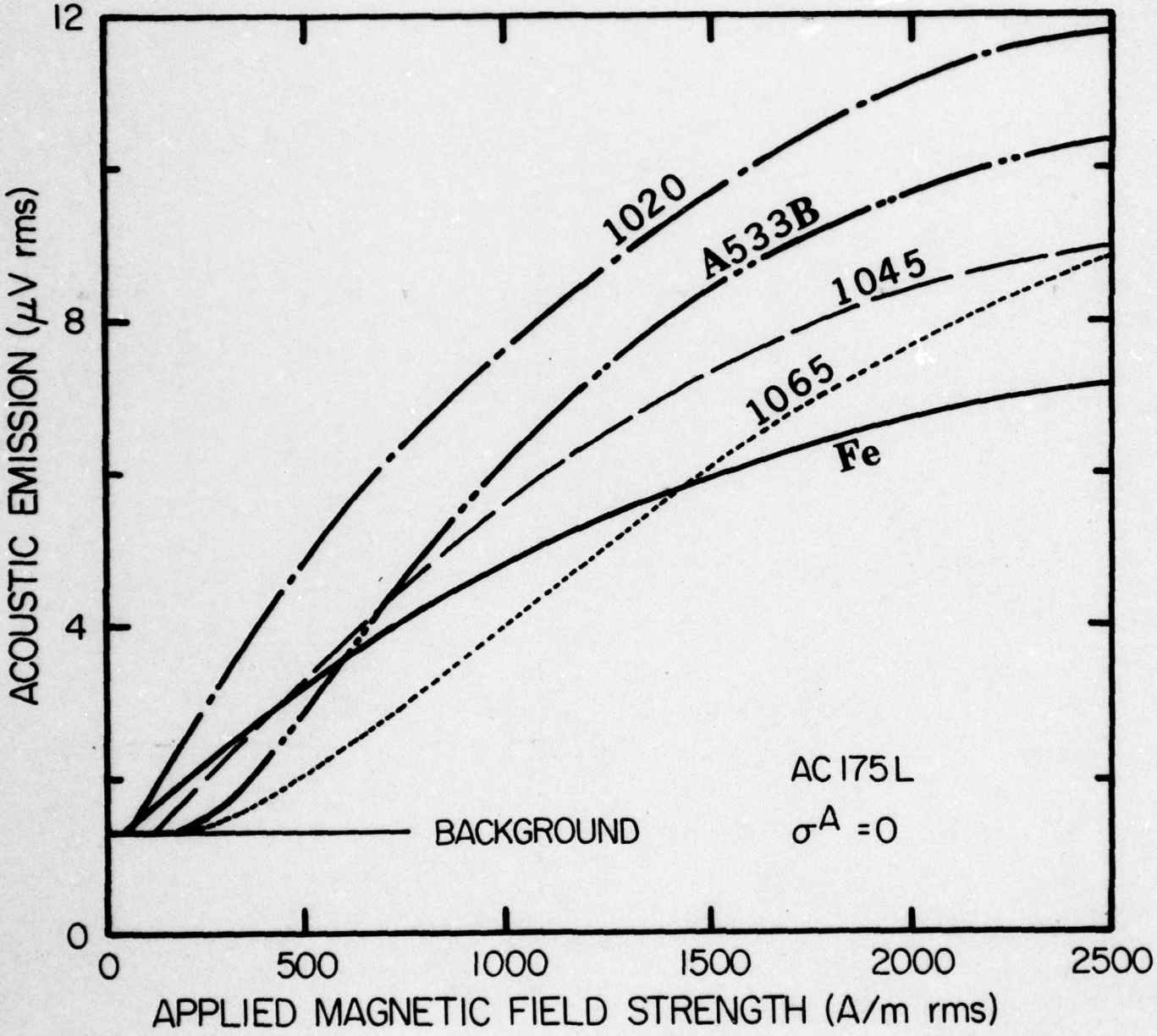

Figure 1. Acoustic emission vs. applied magnetic field strength for five

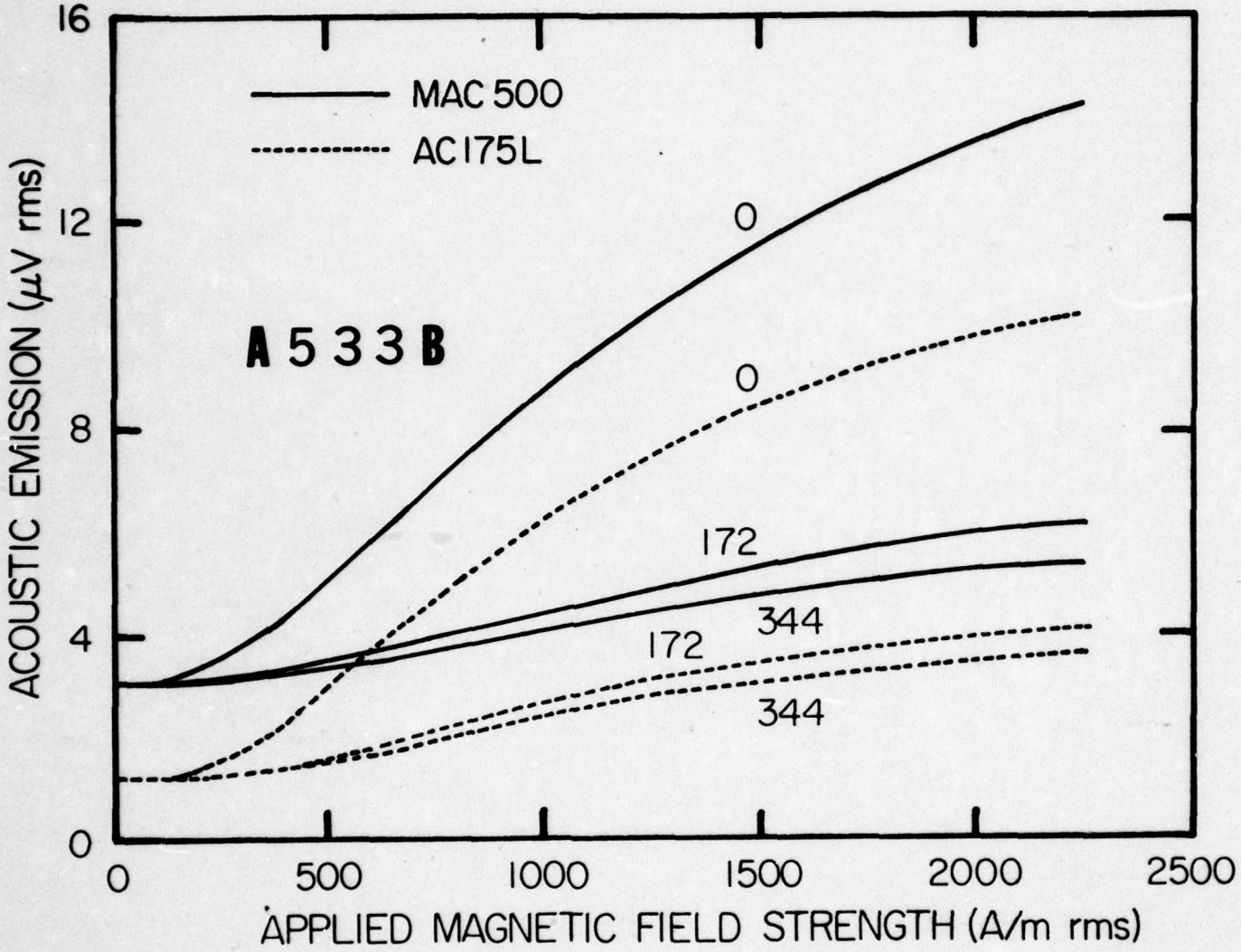

Figure 2. Acoustic emission vs. applied magnetic field strength for A 533 B steel at three stress levels, 0, 172 and 344 MPa. Solid lines for 500 kHz and dotted lines for 175 kHz.

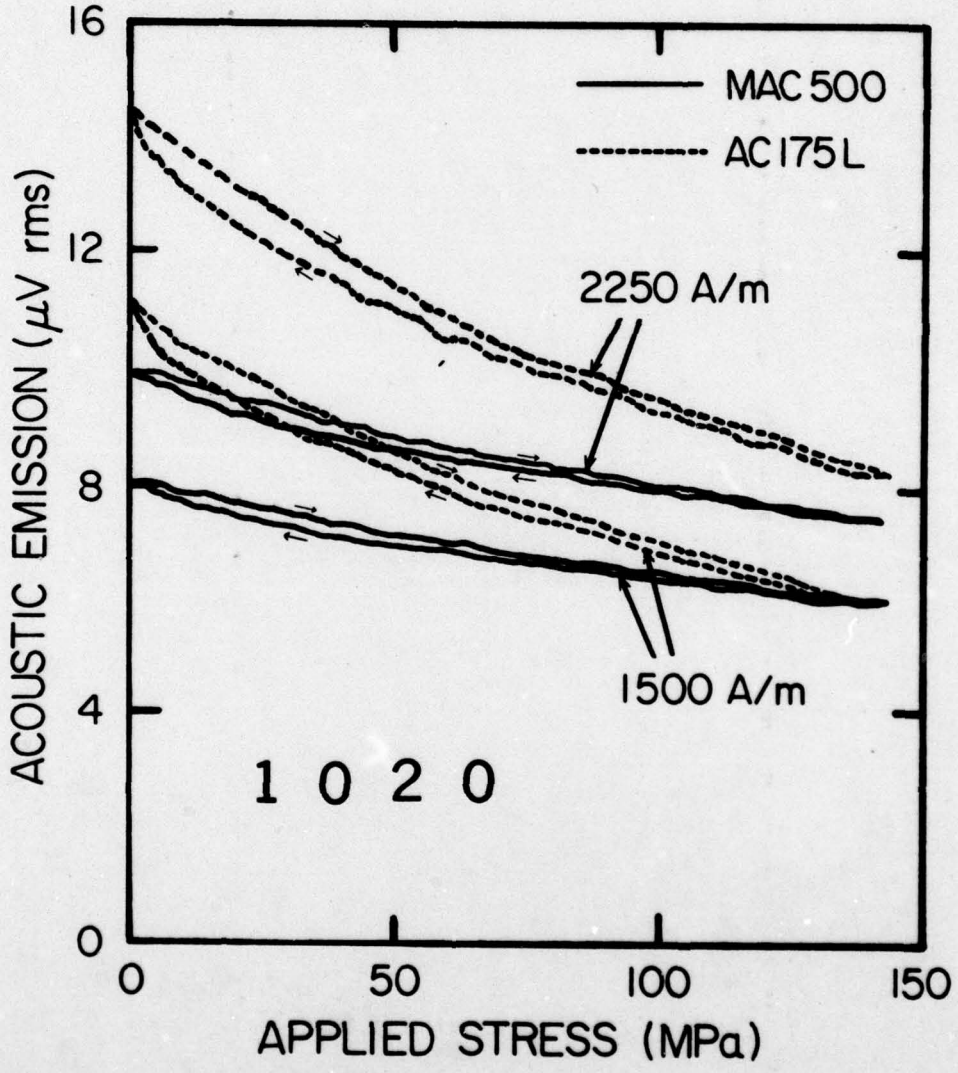

Figure 3. Acoustic emission vs. applied stress for 1020 steel at two magnetization levels. Note the presence of hysteresis in the AE level during loading and unloading.

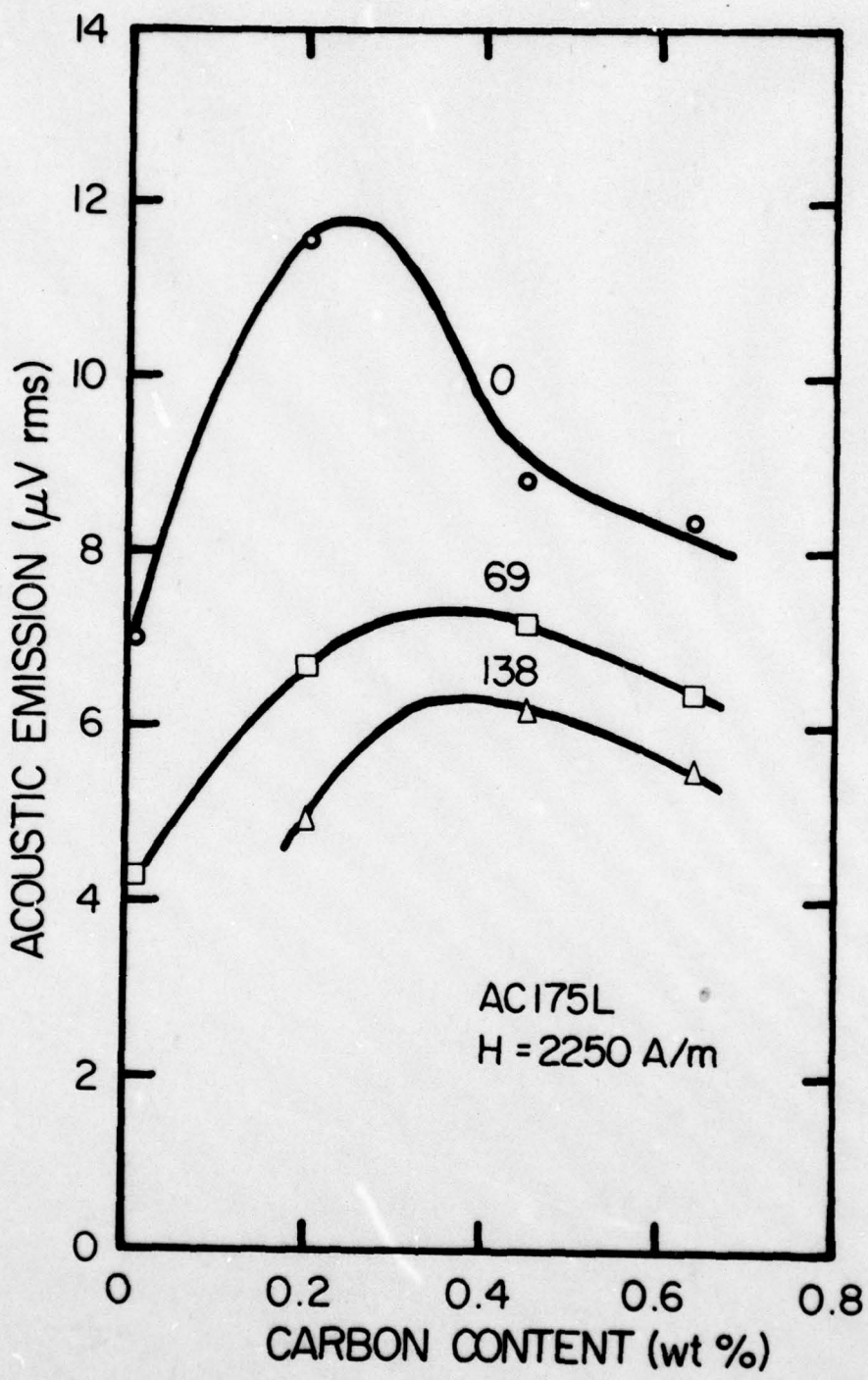

Figure 4. Acoustic emission at three levels (0, 69 and 138 MPa) vs. carbon content of iron and plain carbon steels.

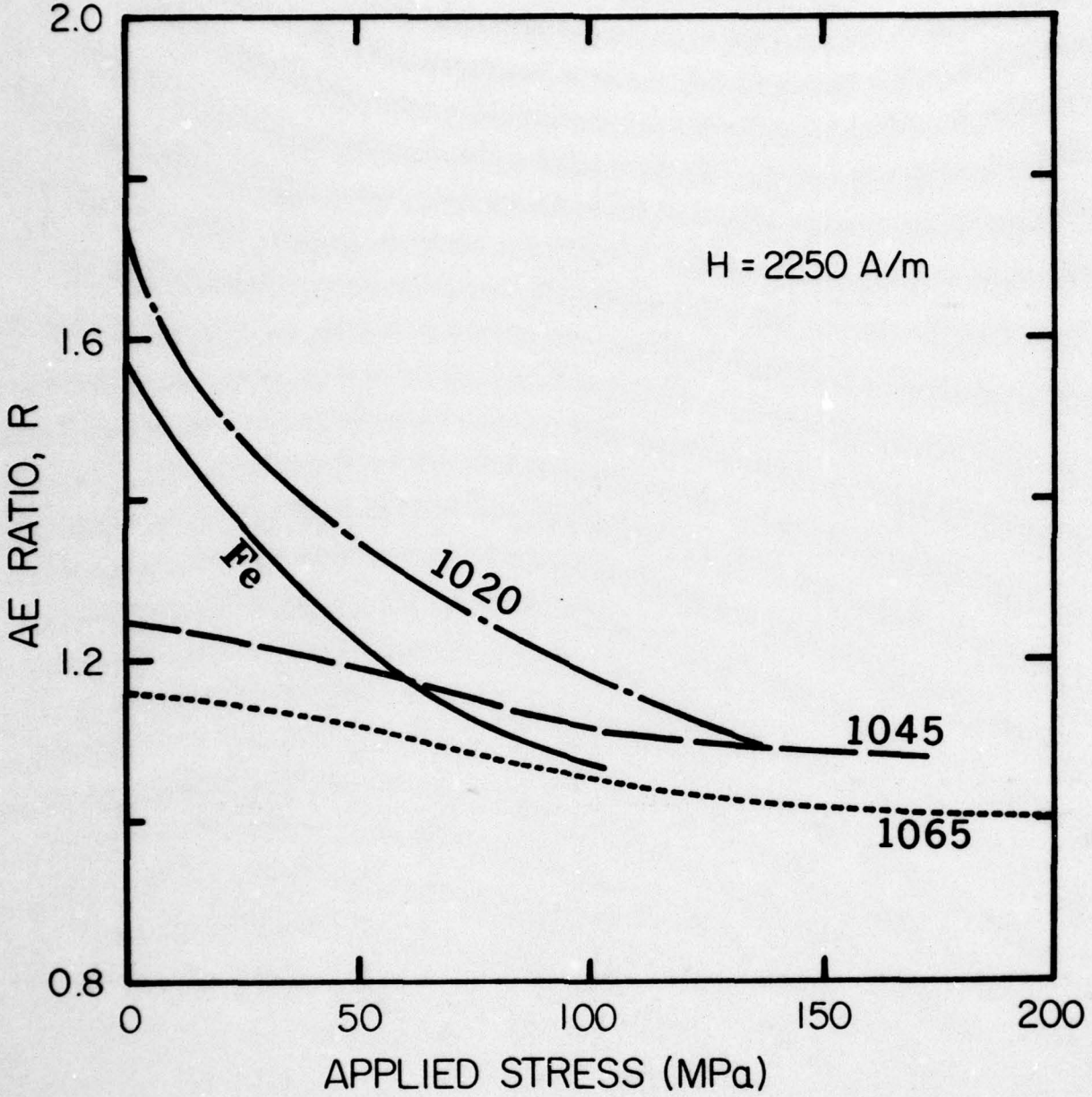

Figure 5. Acoustic emission ratio, R, vs. applied stress for iron and plain carbon steels.

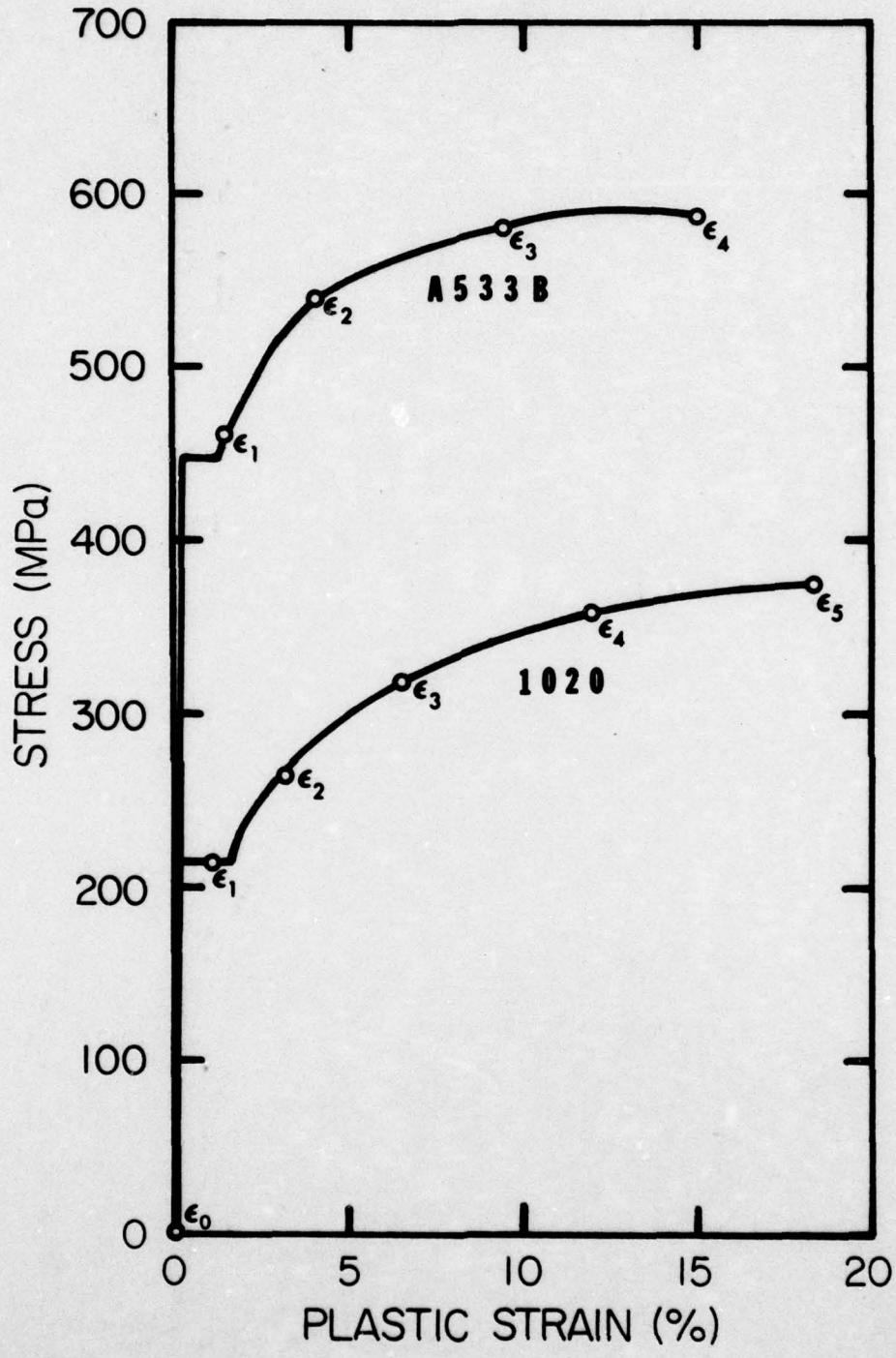

Figure 6. Stress-strain curves of 1020 and A 533 B steels. Circles mark the strain levels where AE measurements were made.

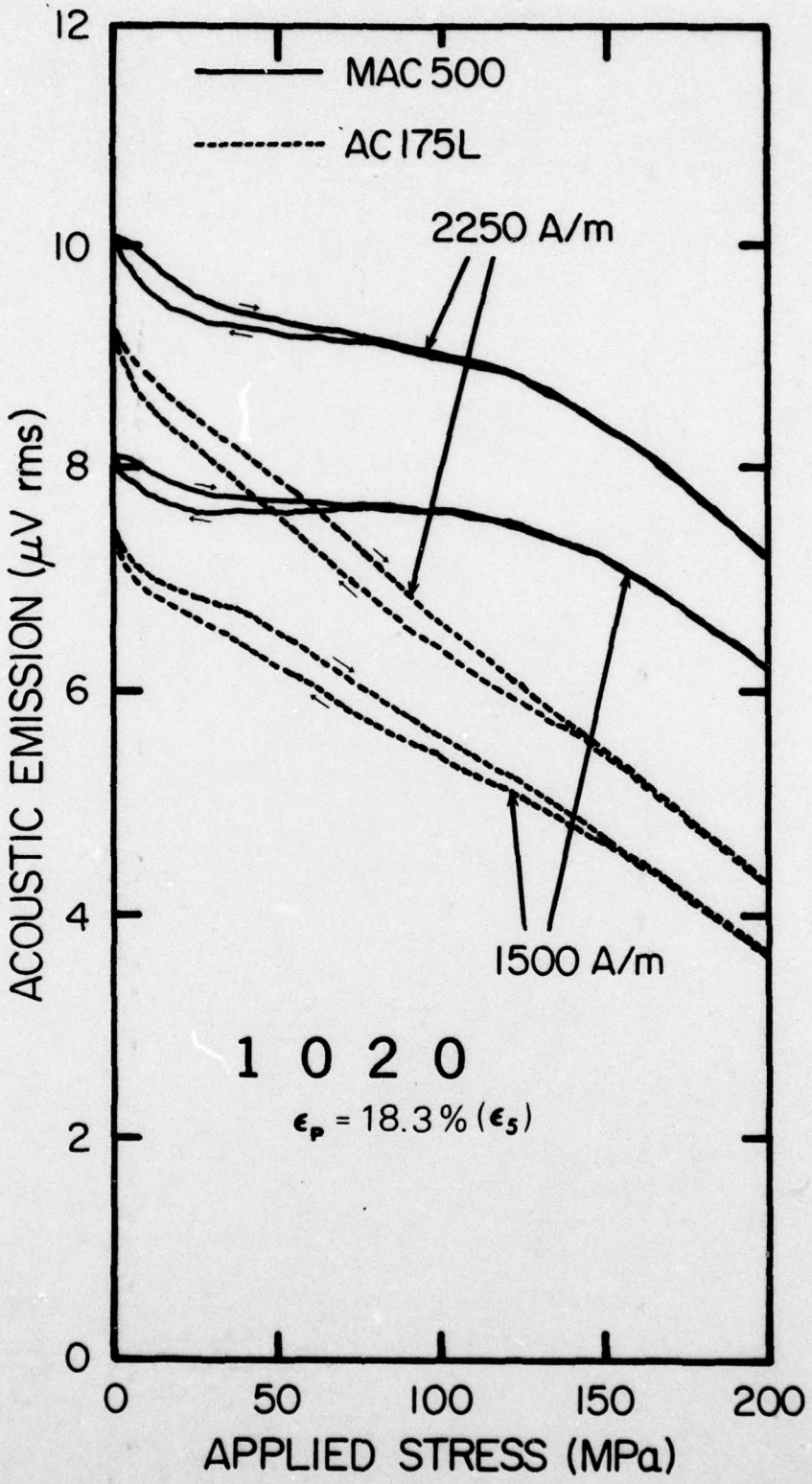

Figure 7. Acoustic emission vs. applied stress for 1020 steel, deformed 18.3%.

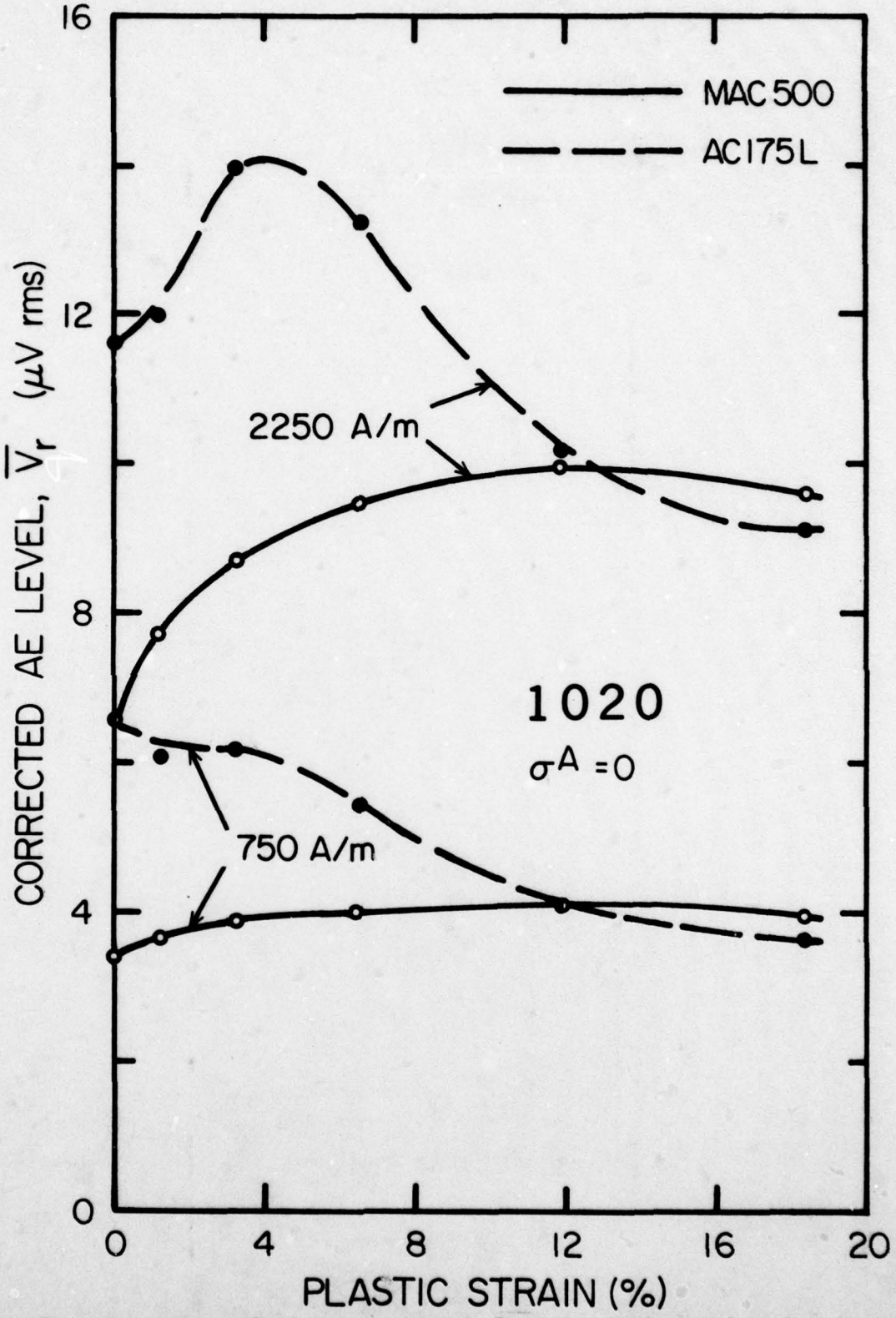

Figure 8. Acoustic emission, corrected for the background noise, against plastic strain for 1020 steel. Applied stress was absent. Magnetization levels are indicated.

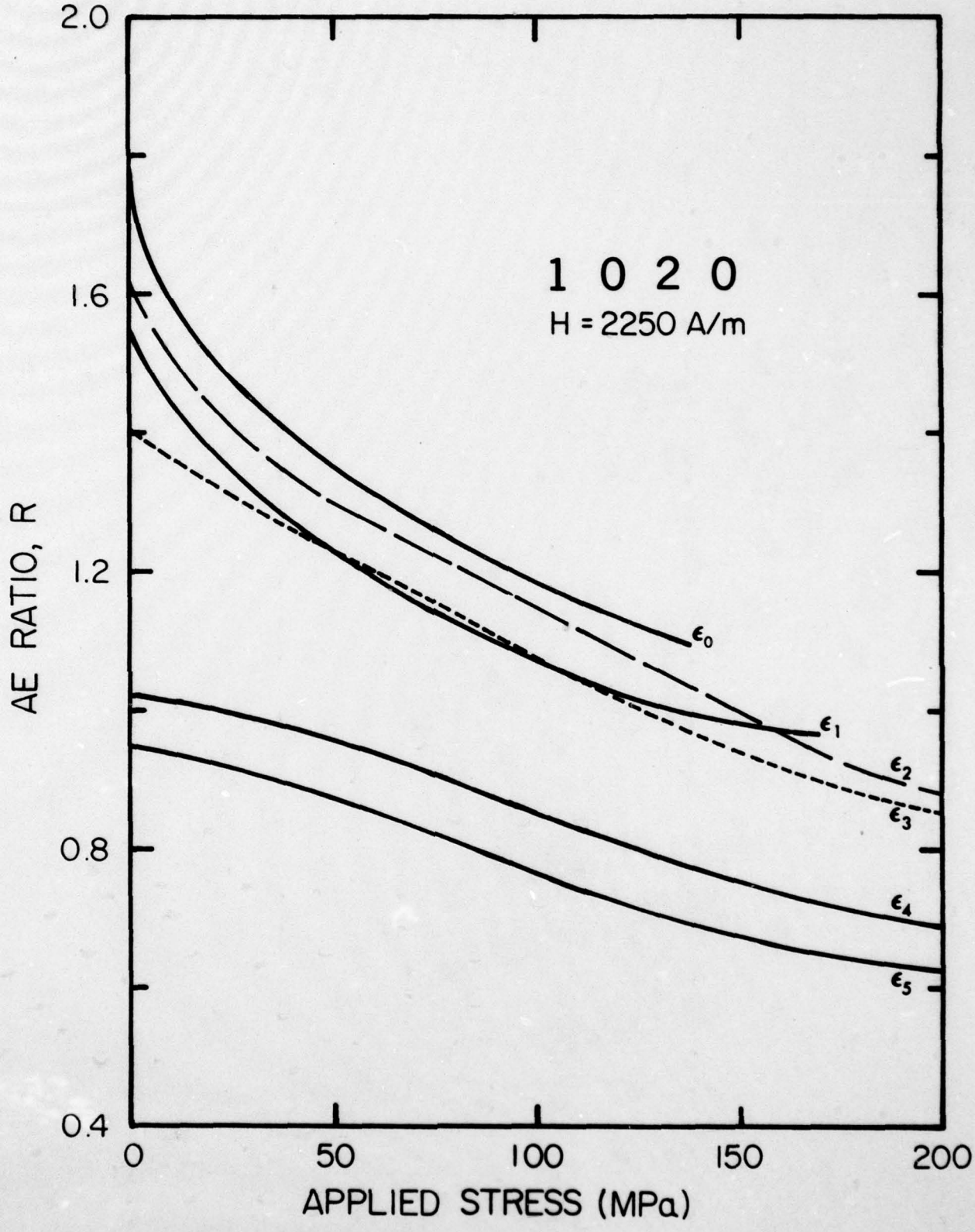

Figure 9. Stress dependence of acoustic emission ratio of 1020 steel at six different levels of plastic deformation.

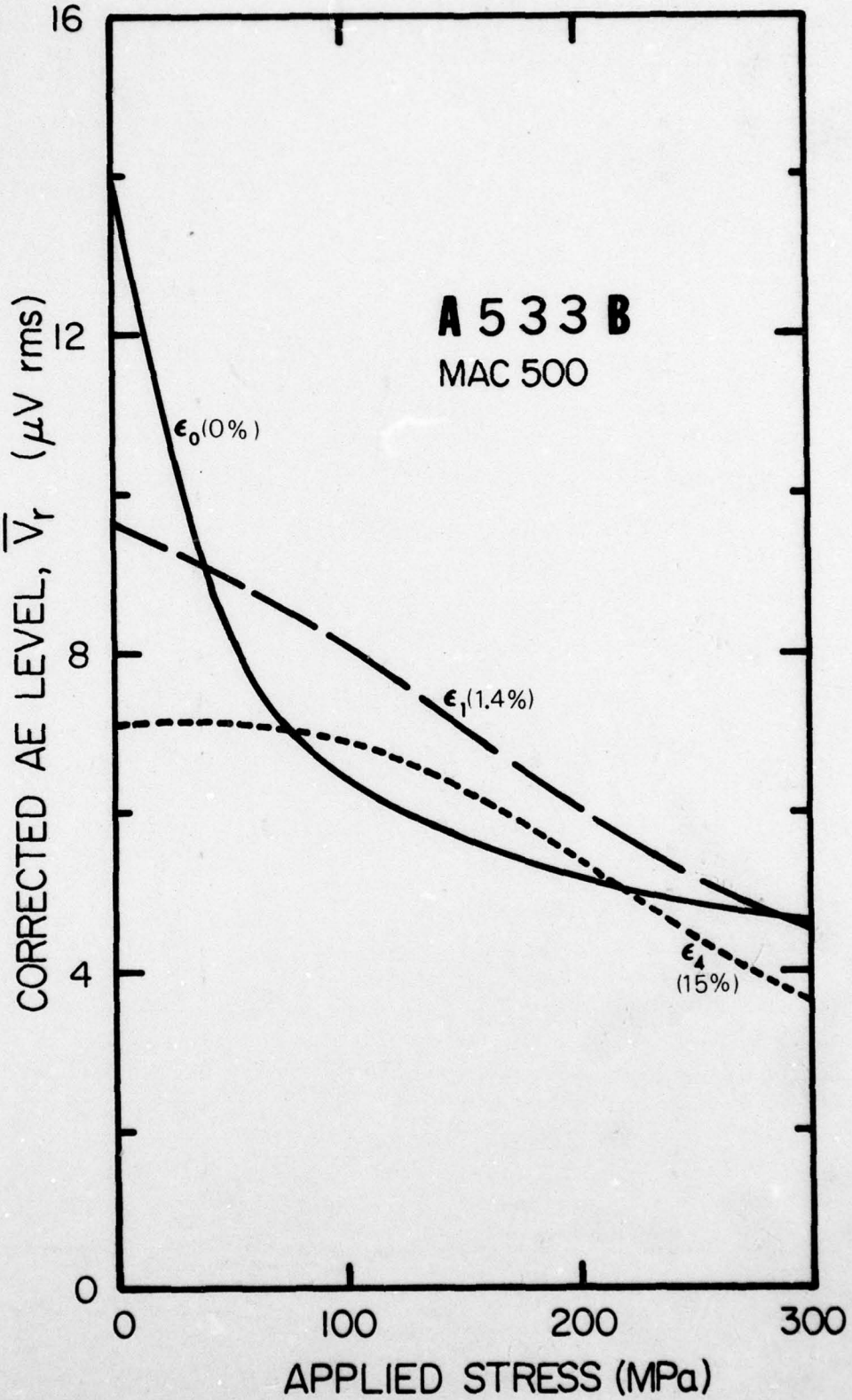

Figure 10. Background corrected AE level (500 kHz) vs. applied stress for A 533 B steel, deformed 0, 1.4 and 15%.

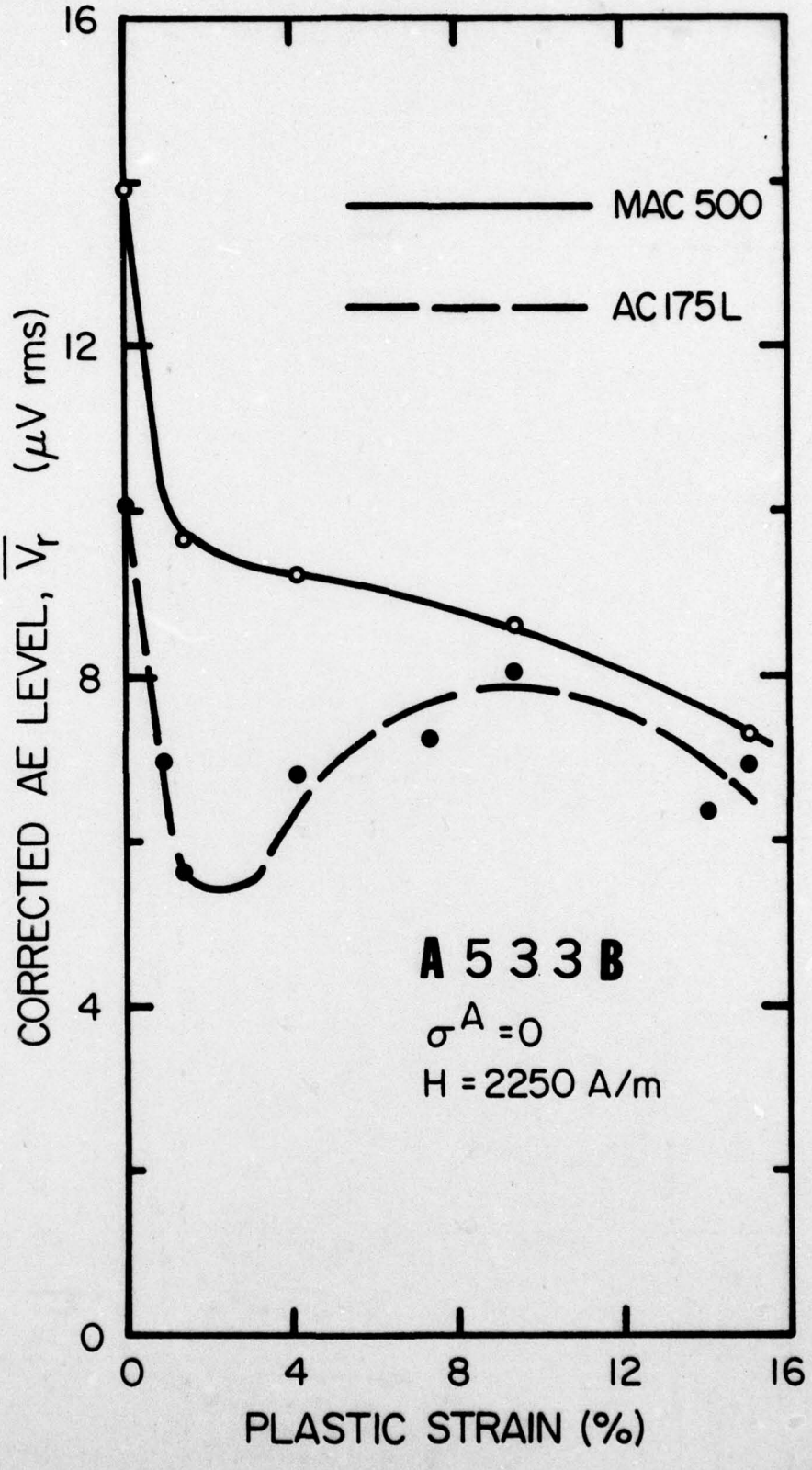

Figure 11. Background corrected AE level as a function of plastic strain for A 533 B steel at zero applied stress.

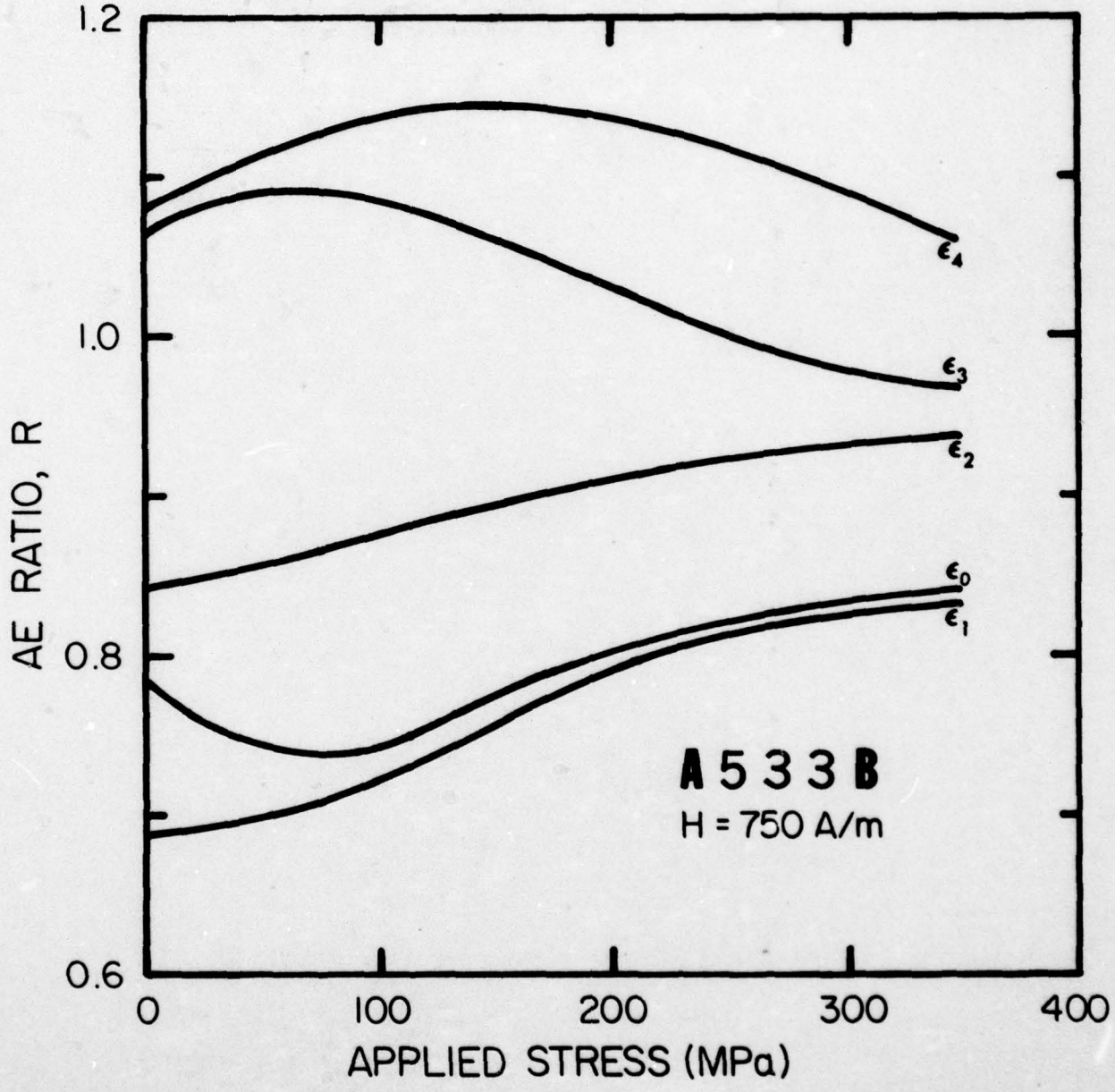

Figure 12. Stress dependence of acoustic emission ratio of A 533 B steel at five different levels of plastic deformation.